



University of  
New Haven

University of New Haven

Digital Commons @ New Haven

---

Master's Theses

Student Works

---

2020

## Investigating the Role of the 5'UTR region of TMEV in Viral Myocarditis

Maryam Alqahtani

Follow this and additional works at: <https://digitalcommons.newhaven.edu/masterstheses>



Part of the [Cell and Developmental Biology Commons](#)

---

THE UNIVERSITY OF NEW HAVEN

Department of Biology and Environmental Sciences

**Investigating the Role of the 5'UTR region of TMEV in Viral Myocarditis**

*A THESIS*

Submitted in partial fulfillment

of the requirements for the degree of

MASTER OF SCIENCE IN CELLULAR AND MOLECULAR BIOLOGY

By:

**Maryam Alqahtani**

University of New Haven

2020

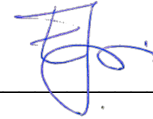
**Investigating the Role of the 5'UTR region of TMEV in Viral Myocarditis**

APPROVED BY



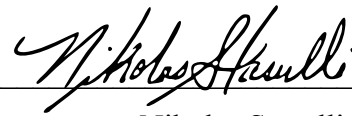
---

Anna Kloc, Ph.D.  
Thesis Advisor  
Assistant Professor, Department of Biology and Environmental Science



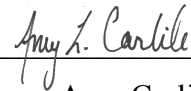
---

Eva Sapi, Ph.D.  
Committee Member  
Professor, Department of Biology and Environmental Science



---

Nikolas Stasulli, Ph.D.  
Committee Member  
Assistant Professor, Department of Biology and Environmental Science



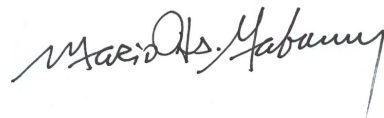
---

Amy Carlile, Ph.D.  
Associate Professor and Chair, Department of Biology and Environmental Science



---

Michael J. Rossi, Ph.D.  
Interim Dean, College of Arts and Sciences  
Professor, Department of Biology and Environmental Science



---

Mario T. Gaboury, J.D., Ph.D.  
Interim Provost and Senior Vice President of Academic Affairs

## ABSTRACT

Viral myocarditis is described as the inflammation of the heart muscle, and it is a common condition that can affect the heart. It is estimated that myocarditis causes 1.5 million deaths annually. In mice, Theiler's encephalomyelitis virus (TMEV) is a common cause of myocarditis. This non-attenuated virus can be used in a cell culture model system to study viral replication and persistence. These processes have been linked to the severity of the heart damage, which in most clinical scenarios, can lead to dilated cardiomyopathy. The 5' untranslated region (5'UTR) found in the viral genome of TMEV is well known to control viral replication. In particular, the internal ribosome entry site (IRES) elements of the 5'UTRs are involved in the replication and translation regulation. In patients suffering from chronic myocarditis, the IRES has been found to acquire deletions, suggesting a strong correlation between mutations, viral persistence and pathogenicity. Similarly, deletions in the 5'UTR secondary loop regions have been linked to increased viral infections. The goal of the research project is to study the 5'UTR region of TMEV to understand its role in viral replication and persistence. During the course of this research project, I designed a cloning strategy to generate four recombinant deletion viruses to test their ability to infect primary cardiac cells. The designed deletions maintained the secondary RNA structures loop, which is important for the recognition of the virus by the host's immune system. In summary, this research will help to better understand the role of 5'UTR elements in regulation of viral replication and its contribution to myocarditis.

## TABLE OF CONTENTS

<b>TITLE.....</b>	<b>1</b>
<b>APPROVAL.....</b>	<b>2</b>
<b>ABSTRACT.....</b>	<b>3</b>
<b>TABLE OF CONTENTS.....</b>	<b>4</b>
<b>LIST OF FIGURES .....</b>	<b>4</b>
<b>INTRODUCTION.....</b>	<b>5</b>
<b>MATERIALS AND METHODS.....</b>	<b>8</b>
<b>RESULTS.....</b>	<b>15</b>
<b>DISCUSSION.....</b>	<b>16</b>
<b>FIGURES .....</b>	<b>19</b>
<b>REFERENCES.....</b>	<b>24</b>

## LIST OF FIGURES

**Figure 1: TMEV RNA viral genome structure**

**Figure 2: Scheme of pDAFI3 plasmid construction**

**Figure 3: Design of deletions in the 5'UTR of TMEV**

**Figure 4: Secondary RNA structure of 5'UTR**

**Figure 5: Digestion of pDAFI3 and pUC75 plasmids**

**Figure 6: Linearization of TMEV RNA**

**Figure 7: Cytopathic effect of TMEV-infected BHK-21**

**Figure 8: Schematic representation of cloning strategy**

## **Introduction**

Human heart disease is the number one killer worldwide, and it is accounted for 17.3 million deaths annually <sup>1</sup>. Heart disease refers to several conditions that can affect the heart, including, but not limited to, coronary artery disease, heart failure, myocarditis, and others. Myocarditis is a heart condition that accounts 1.5 million deaths of the total heart disease conditions globally <sup>2</sup>. The incidence of myocarditis is estimated to be between 10 to 20 per 100.000 people worldwide <sup>3</sup>. Although myocarditis can be caused by several infectious agents (bacteria, fungi, parasites), it is most commonly triggered by viral infections <sup>4,5</sup>.

## **Viral Myocarditis**

Viral myocarditis is an inflammation of the heart muscle (myocardium) that can lead to dilated cardiomyopathy <sup>6</sup>. It can be characterized by a profound infiltration of immune cells as a result of viral infection of the heart <sup>6,7</sup>. Thus, it has been hypothesized to have an autoimmune pathogenesis <sup>8</sup>. The aspects responsible for the initiation and continuation of the immune response are still unclear, but the involvement of infectious agents have been suggested.

Picornaviruses are common etiologic agents for myocarditis <sup>8,9</sup>. Recent studies have shown that a viral infection of cardiomyocytes is required for the development of myocarditis and subsequent cardiomyopathy <sup>6,10</sup>. Viral infections can cause significant damage to cardiomyocytes through direct injury and secondary immune reactions, leading to acute and subacute phases of myocarditis <sup>11,12</sup>. Of special interest is the observation that 35%-50% of patients with myocarditis developed a persistent enteroviruses infection of the heart, which is associated with the heart damage in the chronic phase of the disease, leading to dilated cardiomyopathy <sup>3</sup>. This demonstrates that the viral infection of cardiomyocytes is an important step that determines the pathogenesis and persistence of the virus during a systemic infection. Coxsackievirus group B3 (CVB3) is a

good example of enterovirus-induced myocarditis in humans and it is detected in 20%-30% of all viral myocarditis related cases<sup>13</sup>. The isolation of CVB3 RNA genome from a heart tissue taken from patient with DCM showed deletions of 15 to 48 nucleotides in the 5' untranslated region (5'UTR) of the viral genome, suggesting a strong association between deletions within the 5'UTR and viral virulence<sup>14</sup>. Those deletions were characterized by a low viral RNA load (8.10 (2)copies/ $\mu$ g of nucleic acids), leading to viral persistence and DCM<sup>14</sup>. It is well-documented that the 5'UTR regulates viral replication, so deletions within this particular region were presumed to be associated with chronic myocarditis<sup>14,15</sup>. Moreover, many picornaviruses are known to cause myocarditis, with similar mechanisms and complications in humans, in experimentally inoculated mice, as shown in Theiler's Murine Encephalomyelitis Virus (TMEV) model system<sup>13,16,17</sup>.

TMEV is a non-enveloped positive single-stranded RNA virus belonging to the *Cardioviruses* genus of Picornaviruses. It is a natural pathogen in mice that can cause myocarditis through direct damage to cardiomyocytes, which is similar to human cases of myocarditis<sup>17,18</sup>. Omura *s. et al.* have revealed cardiomyocyte damage in TMEV-infected mice groups that was characterized by high troponin I levels and high viral RNA loads at 4 days post-infection ( $r=0.79$ ;  $P<0.05$ )<sup>18</sup>. In addition to the similar mechanisms of disease initiation, DA strain of TMEV was proven to induce triphasic myocarditis, and to imitate clinical and immunological findings in human CVB3-induced myocarditis<sup>17,18</sup>. The DA strain sequence was found to be more closely related to members of the *Cardiovirus* genus than to members of other Picornavirus genera<sup>19</sup>. The intraperitoneal infection of C3H mice with TMEV (DA strain) lead to an infection of the heart and the development of the three phases: acute, subacute, and chronic<sup>20</sup>. The acute phase was characterized by viral pathology inducing innate immune response, and the subacute phase was characterized by the antiviral immune responses and autoimmunity that lead to more damage of

the myocardium<sup>20</sup>. As a result of heart damage during the acute and subacute phases, cardiac remodeling was revealed as a dominant event of chronic phase<sup>20</sup>. Moreover, susceptibilities to TMEV-induced myocarditis were shown to differ among mouse strains. The most highly susceptible strain was the C3H strain and the intermediate susceptible strain was the C57BL/6. However, a highly resistant strain was the SJL/J<sup>18,20</sup>. It was demonstrated that TMEV-infected C3H mice developed all three phases, while SJL/J mice developed only the acute phase and C57BL/6 mice developed both acute and subacute phases<sup>18,20</sup>. The different susceptibilities to viral myocarditis were dependent on the genetic background of each mouse strain, and that has also been demonstrated in humans<sup>21</sup>. With information given, it can be said that several aspects of TMEV-induced myocarditis have been reported in scientific literature allowing the establishment of TMEV as a model system to study myocarditis in 2014<sup>18,17</sup>. Those aspects focused on showing the similarities between TMEV and its homologs in humans in regards to myocarditis molecular mechanisms, immunological and clinical findings, and host suitability, shedding the light on using TMEV as a model system to further understand human viral myocarditis. Most importantly, TMEV translation and replication was shown to be controlled by the 5'UTR as in most Picornaviruses<sup>22</sup>. However, the role of genetic regions of TMEV genome in viral infection or persistence in myocarditis in mice was not given much attention.

The TMEV genome is 8093 nucleotides long with a poly(A) tail and it has a 5' UTR that stretches from nucleotides 1 to 1065. The 5' UTR contains highly structured stem-loops that were shown to be conserved throughout *Cardioviruses* (Figure 1)<sup>23</sup>. This suggests the importance of these loops in regulating viral replication within the cardiomyocytes during heart infection, which possibly leads to viral persistence in the heart. Therefore, studying the 5'UTR region of TMEV might help identify important regions that can mediate viral infection and the likelihood to cause



damage in primary cardiac cell lines. Also, manipulating the TMEV genome by introducing deletions in the 5' UTR region might help to determine the effect of these deletions on viral persistence by measuring the immune response of viral mutant TMEV-infected cardiac cell lines. Most importantly, using TMEV to investigate the role of genetic regions in the 5'UTR will further our understanding of human myocarditis by defining similar regions in the CVB3 genome.

## **Material and Methods**

### **Plasmids**

#### *TMEV cDNA*

The full TMEV sequence was cloned into a full-length pDAFI3 cDNA vector, which was kindly obtained from Dr. Rymond P. Roos' lab from the University of Chicago. The pDAFI3 plasmid contained a T7 promoter, recognition sites for XhoI, ClaI, and XbaI restriction enzymes, Amplification region, and the viral cDNA downstream of the T7 promoter (Figure 2).

#### *Deletion construct*

The desired deletion sequence in the 5'UTR region of TMEV was cloned into pUC75 plasmid, and was ordered from BioBasic company.

### **Cell lines**

#### *BHK-21 Cell lines*

The Baby Hamster Kidney (BHK-21) cell line was kindly provided by Dr. John Rose (Yale University, New Haven, Connecticut). The BHK-21 were maintained in Dulbecco modified Eagle medium (DMEM) containing 10% Calf serum (iron supplemented) + 1% glutamine/penicillin/streptomycin. The cells were passaged every 48 hours according to standard cell culture passing protocol.

### *MCM cell lines*

The Mouse Cardiac Myocyte (MCM) C57BL/6 (primary cardiac cell line for TMEV viral infection) were ordered from ScienCell Research Laboratories. The MCM cell lines were maintained in Mouse Cardiac Medium-serum free media (ordered from ScienCell Research Laboratories). The cells were passaged every 72 hours according to the standard cell culture passing protocol.

### *Cell culture passaging protocol*

All cell cultures were maintained at 37°C and in 5% CO<sub>2</sub> incubator. Briefly, cells were washed with 3mL PBS (2x). Then, 0.5mL Trypsin was added, and flasks were incubated at 37°C for 2 minutes to detach the cells. 4ml of DMEM media was added and cell suspension was transferred into a 15ml falcon tube and centrifuged for 5 minutes at speed of 4400 rcf. Then, media was removed without disrupting the pellet and 5mL of fresh media was added. The cells were counted by adding 10µl of cell suspension and 10µl TrypanBlue in a new Eppendorf tube. The cells were plated (based on calculations) in new T-25 flasks.

## **Generation of mutant TMEV**

### *Primer design*

Primers were designed to flank deletions in the 5'UTR region that varied in size to generate four different recombinant TMEVs (Figure 3A). The first deletion construct was designed to flank the desired sequence of 20 nucleotides. The subsequent constructs contained deletions of 40 nucleotides (RVA40), 60 nucleotides (RVA60), and 84 nucleotides (RVA84) (Figure 3B).

### *mFOLD program*

mFOLD program was used to create the deletions in the 5' UTR region of the TMEV. The program allows to estimate the formation of the secondary RNA structure and the confirmation of preserving the single loop structure of loop A in the 5'UTR.

### *Bacterial Transformation*

Bacterial transformation was carried out to amplify pDAFI3 and pUC75 plasmids. Briefly, 1µl of plasmid was added to 50µl of *E.coli* competent cells and placed on ice for 30 minutes. Then, the *E.coli* competent cells were heat-shocked at 42°C for 30 seconds and placed back into ice for 1 minute. 300 µl of Super Optimal Broth (S.O.C) was added to obtain maximal transformation efficiency of *E. coli*. The tubes were incubated on a shaking platform of a 37°C incubator for 1 hour. 100µl of mixtures were plated onto LB agar plates with ampicillin (100 µg/mL) and the plates were incubated for 24 hours at 37°C.

The next day, the transformed bacterial colonies were grown in liquid cultures of 2mL LB broth and 2 µl of 1000x ampicillin stock (100 mg/ml). The bacterial growth tubes were incubated on a shaking platform of a 37°C incubator for 24 hours.

### *DNA isolation protocol*

The plasmids were purified using a phenol:chloroform:IAA extraction (SigmaAldrich). Briefly, 1.5 mL of bacterial culture was transferred into a new Eppendorf tube and centrifuged for 5 minutes at 14,000 rpm. The supernatant was discarded, and the pellet was resuspended in 50µl of TE buffer (the buffer contains 10 mM Tris-HCl, pH 8 and 1 mM EDTA), 300µl TENS lysis buffer (500ml buffer contains 5 mL 1M Tris-HCl pH 8.0, 12.5 mL 20% SDS, 5 mL 10N NaOH, 477.5 mL H<sub>2</sub>O), and 100µl of sodium Acetate (3M NaAc pH 5). The tube was centrifuged for 5 minutes at top speed 14,000 rpm, and cells were transferred into a new Eppendorf tube. 1µl RNase

A was added and tube was incubated at 37°C for 15 minutes. Then, 600µl of phenol:chloroform:IAA was added to the mixtures and centrifuged for 10 minutes at 14,000 rpm. The upper layer was removed and transferred to new Eppendorf tubes. 200µl of 100% ethanol was added and tube was centrifuged for 10 minutes at 14,000 rpm. The supernatant was discarded and 100µl of 70% ethanol was added and centrifuged for 10 minutes at 14,000 rpm. The supernatant was discarded and the pellets were resuspended in 50µl of water. The final concentration was measured using Nanodrop.

#### *Restriction enzyme digestion*

The pDAFI3 and pUC75 plasmids were digested using XhoI and ClaI enzymes (New England Biolabs) by setting up two reactions. The first reaction was the pDAFI3 reaction and it was prepared by adding 5µl of CutSmart buffer, 1µl of ClaI restriction enzyme, 1µl of XhoI restriction enzyme, 10µl of DNA, and 33µl of nuclease-free water. The second reaction was the pUC75 reaction and it was prepared by adding 5µl of CutSmart buffer, 1µl of ClaI restriction enzyme, 1µl of XhoI restriction enzyme, 10µl of DNA, and 33µl of nuclease-free water. The reactions were incubated at 37°C for 3 hours.

#### *Dephosphorylation of 5'-end*

Dephosphorylation of 5'-end step was carried out to avoid self-ligation of pDAFI3, using quick dephosphorylation kit (M0508) (New England Biolabs). According to the manufacturer's protocol, a reaction of 20 µl was prepared by adding 2µl of CutSmart Buffer (10X), 1 µl of rSAP (Shrimp Alkaline Phosphatase) (New England Biolabs), and 18µl of water. The mix reaction was incubated at 37°C for 30 minutes, followed by inactivation of the reaction at 65°C for 5 minutes.

### *Restriction enzyme digestion*

Single digestion was carried out to ensure the efficacy and validity of the restriction enzymes (ClaI and XhoI) using only pDAFI3 plasmid. Two reactions were set up: reaction 1 contained 5µl of CutSmart Buffer, 1µl of XhoI restriction enzyme, 2µl of TMEV cDNA, and reaction 2 contained 5µl of CutSmart Buffer, 1µl of ClaI restriction enzyme, 2µl of TMEV cDNA. The two reactions were incubated at 37°C for 3 hours.

### *Agarose gel electrophoresis*

An agarose gel (0.8%) was prepared to run the digestion reactions from the restriction enzyme digestion experiments. To prepare the gel, 0.8 grams of agarose gel powder was mixed with 100 ml of TAE buffer and the mixture was heated using microwave for 2 minutes. Then, when the solution cooled down, 3µl of SYBR Green Safe dye (Invitrogen) was added. The gel was allowed to solidify in the gel dock for about 20 minutes. To prepare samples, the following reactions were mixed: 2µl of cDNA plasmid, 2µl of 6x Loading dye, and 6 µl H<sub>2</sub>O. The prepared samples for the single digestion reactions of pDAFI3 and the double digestion reactions of pDAFI3 and pUC75 were loaded into the wells, and the gel was run for 40 minutes. The bands were visualized using a gel imaging system. The concentrations was measured using a Nanodrop.

### *Gel extraction*

The right bands sizes from the double digestion of pDAFI3 and pUC75 were extracted from the gel using QIAquick gel extraction kit (50) (Cat. No. 28704 from QIAGEN). According to the manufacturer's protocol, the extracted gel slice was weighted. Then, 300µl of Buffer QG to 100µl was added to each digestion reaction and placed in water-bath set to 50°C for 10 minutes until the gels were completely dissolved. 100µl of isopropanol was added to the reactions and reactions were transferred into provided QIAquick spin columns and centrifuged for 1 minute. The

flow-through was discarded and the QIAquick spin column was placed back into the collection tubes. Then, 500µl of Buffer QG was added to the QIAquick spin column and centrifuged for 1 min. The flow-through was discarded and 700µl of Buffer PE was added and the QIAquick spin column and centrifuged for 1 min. The flow-through was discarded and the QIAquick spin columns were placed into clean 1.5ml microcentrifuge tubes. The digested cDNA was eluted in 30µl water.

#### *PCR purification*

The pDAFI3 samples from the single digestion were purified using QIAquick PCR Purification Kit (Cat. No.28104) (QIAGEN) according to the manufacturer's protocol.

### **Generation of TMEV RNA**

#### *Restriction Enzyme Digestion*

The original TMEV cDNA plasmid was linearized by carrying out a single restriction enzyme digestion using XbaI restriction enzyme. The digestion reaction was set up by adding 5µl of CutSmart Buffer, 2µl of XbaI Restriction Enzyme, 5.7µl of TMEV cDNA and 37.3µl of nuclease-free water.

#### *Agarose gel electrophoresis*

Agarose gel (0.7%) was prepared to run samples from the digestion of the TMEV cDNA. The samples were prepared by adding 2µl of TMEV cDNA plasmid, 2µl of 6x Loading dye, and 6 µl H<sub>2</sub>O. The control sample was prepared by adding 6µl of wild-type TMEV cDNA plasmid, 2µl of 6x Loading dye, and 4µl of H<sub>2</sub>O. The samples were loaded into the gel, and bands were visualized using a gel imaging system. The concentrations was measured using a Nanodrop.

#### *In-vitro RNA transcription*

*In-vitro* RNA transcription was carried out to produce an RNA transcript from the linearized TMEV cDNA template. pDAFI3 TMEV-cloned vector included T7 promoter that is

recognized by T7 RNA polymerase, which was used to reverse transcribe the TMEV cDNA to RNA using T7 RiboMAX™ Express Large-Scale RNA Production System kit (Cat No./P1320) (Promega). The Reaction was prepared according to the manufacturer's protocol (Synthesizing Large Quantities of RNA protocol) by adding 10 µl of RiboMAX Express buffer, 8µl of linear TMV cDNA template, 2 µl of T7 Express Enzyme Mix. The reaction was mixed and incubated at 37°C for 30 minutes. Then, 1µl of RNase-free DNase was added the *in-vitro* transcription reaction and incubated for 15 minutes at 37°C.

The linearized TMEV cDNA was purified using a Monarch RNA Cleanup kit (500 µg) (Cat.No.T2050S) (New England BioLabs). According to the manufactures' protocol, 100µl of RNA Cleanup Binding Buffer was added to the *in-vitro* transcription reaction with the linearized TMEV cDNA. 150 µl of ethanol (100%) was added and mixed and the sample was loaded onto a provided column tube and span down for 1 minute at top speed 14,000 rpm. The flow-through was discarded and 500µl RNA Cleanup Wash Buffer was added and span down for 1 minute at top speed 14,000 rpm (2x). The column was transferred into RNase-free 1.5 microfuge tube and the sample was eluted in 50µl water and incubated at room temperature for 5 minutes and span down for 1 minute at top speed 14,000 rpm (2x). The concentration was measured using Nanodrop.

#### *RNA Electroporation*

TMEV RNA was generated by infecting BHK-21 cells along with repeated passaging, following standard viral passaging and electroporation protocols. Briefly, BHK-21 cells were resuspended in 4ml PBS and centrifuged for 5 minutes at top speed. PBS was discarded and the cell pellet was resuspended in 1ml PBS (2x). In electroporation Cuvette, 500µl of BHK-21 cells was added to 10µl of purified TMEV RNA. The Cuvette was placed into an electroporation

machine and pulsed with 300 volts. Finally, the mix was transferred into a prepared T-25 flask containing 5ml of fresh iron-supplemented DMEM media and incubated at 37°C overnight.

## **Results**

### **1. Derivation of mutant TMEV (RVA20)**

#### *Confirmation of preserved single loop structure of the 5' UTR region of the TMEV*

The mFOLD program showed that the deletions created in the 5'UTR of TMEV did not alter the single loop structure of the loop A in the 5'UTR region. The mFOLD program showed that deletion created in loop A to generate the four recombinant viruses was preserved (Figure 4).

#### *Restriction enzyme digestion*

Digestion of pDAFI3 plasmid (10.8 kb) was successful and resulted in two bands that corresponded to 2 kb (contained the 5'UTR region) and 8.8 kb (contained the remaining sequence of TMEV cDNA). The digestion of pUC75 (3.2 kb) plasmid resulted in two bands that corresponded to 2 kb (the deletion construct) and 1.2 kb (the remaining sequence of the pUC75 plasmid). The single digest products of pDAFI3 cut with XhoI and the pDAFI3 cut with ClaI showed a size of 10.8 kb compared to the control of wild-type pDAFI3 plasmid (Figure 5).

#### *Dephosphorylation of pDAFI3 plasmid*

The pDAFI3 plasmid was dephosphorylated, and no colonies were observed on the LB agar plates supplied with ampicillin after bacterial transformation.

### **2. Generation of TMEV RNA**

#### Linearization of pDAFI3 plasmid

The single digestion of the pDAFI3 plasmid (containing TMEV cDNA) with the XbaI restriction enzyme was successful and I was able to visualize a linearized TMEV cDNA product



on the agarose gel. The linearized TMEV cDNA was shown as a sharp band of a size 10.8kb, and was compared to the band of the control, non-linearized wild-type TMEV cDNA (pDAFI3) (Figure 6).

#### *The effect of TMEV RNA infection of BHK-21 cell lines*

BHK-21 cells were observed for cytopathic effect to determine the cells death as an indication of TMEV RNA growth in those cells. BHK-21 showed a change in morphology where they had rounded-shape or they were floating on the surface of the T-25 flask. In comparison, the normal BHK-21 cells showed epithelial morphology and were attached to the surface of the flask, indicating no viral infection (Figure 7).

### **Discussion**

My research project focuses on studying the conserved loops of the 5' UTR of the TMEV. My goal was to develop a strategy to generate four recombinant TMEV viruses with a 20, 40,60, and 84 nucleotides deletions and test these viruses for growth. I was able to design deletions that would preserve the secondary loop structure using the mFOLD program. This was important as any alterations to secondary RNA structures may impact the viral recognition by the immune system. Furthermore, I was able to design a restriction enzyme strategy to replace a 2kb TMEV genomic region flanked by XhoI and ClaI restriction enzymes with a viral deletion construct (Figure 8). In the future, this deletion construct will be used to create recombinant viruses and test their growth in BHK-21 cell line and a primary cardiac cell line. Consequently, this research will reveal the role of 5'UTR of TMEV in viral replication, viral resistance, and pathogenicity.

The 5'UTR region of viruses is known to be associated with viral replication, translation and pathogenicity. Among Picornaviruses, there is a high degree of sequence conservation in the 5'UTR region. Furthermore, the 5'UTRs often form secondary structures, such as loops, clover-

like structures, or pseudoknots. These structures have been implicated in viral replication and stability. Interestingly, they may also play a role in the infection cycle of the virus. There are well-documented examples of viruses with deletions in the 5' UTR regions that make the virus more potent and more likely to infect tissues that are not normally associated with the primary site of infection. For example, loss of nucleotides 1-22 and 1-25 out of the CVB2 cloverleaf increases the likelihood of the virus to infect a human heart tissue, and result in myocarditis<sup>24</sup>. Furthermore, persistent viral populations that belong to the CVB3 virus have been reported to contain up to 48 deletions in the 5'UTR region of the viral genome.<sup>14</sup>

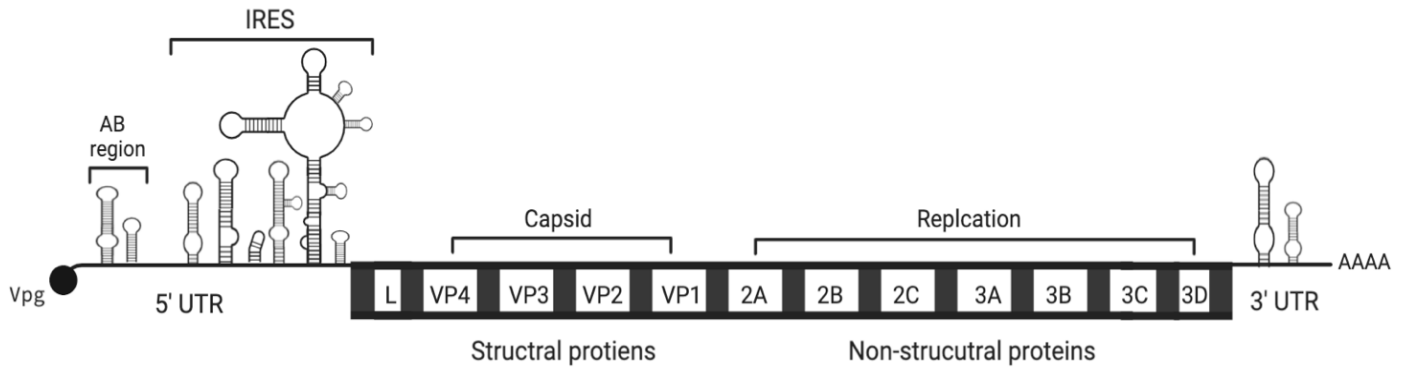
It is very important to dissect the role of mutations in the 5'UTR region of viral genomes, and their impact on viral pathogenicity, as it is related to the function of human heart. It is known that the heart can get infected by viruses, and that these viral infections can cause a permanent heart damage. On the other hand, diagnosing heart infections is complicated because of the location of the heart. Therefore, studying the function of the 5'UTR of the virus genome can help us understand the disease process associated with the viral infection. Particularly, inducing deletions in the 5'UTR can offer insight into the processes associated with viral replication, translation, and viral potency.

In future experiments, the described research will be important for assessing why certain viral mutations or deletion can have an impact on viral replication and heart function. To facilitate these analyses, the BHK-21 cell line will be infected with the mutant TMEV containing the induced deletion in the 5' UTR, and testing for viral growth through the measurement of viral titer using a TCID50 method. The other three designed TMEV 5'UTR deletions will also be generated in the BHK-21 cell line and tested for growth and the ability to cause infection. All viruses generated will be used to produce viral stocks. Briefly, the viruses will be grown in the BHK-21

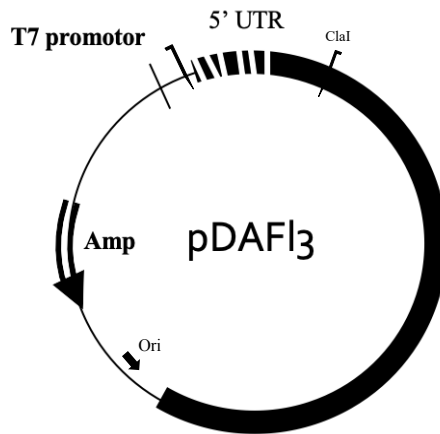
cells for a couple of passages. A titer assay will be performed, and viral pegylation will be used to concentrate all viruses. The viruses will be tested in a primary cardiac cell line (Mouse Cardiac Myocyte MCM). The same concentration of each virus will be used to infect the primary mouse myocyte cells. After CPE is established, the host genetic material (DNA and RNA) will be extracted. The host RNA will be reverse transcribed to cDNA, which will be used for quantitative PCR assays. Specifically, the regulation of the innate immune system genes will be measured to assess the response against each virus. I expect to observe differences in the immune gene expression in response to each virus.

The results obtained in course of these studies will generate a model system to analyze the role of the 5'UTR deletions in the TMEV genome in cardiac cell infection. In the future, the knowledge of the 5'UTR important regions might provide better diagnostic tools for patients suffering from virus-induced heart disease. For example, a sequencing analysis might be performed on people presenting heart disease symptoms to determine if there are any viruses with 5'UTR deletions in their hearts.

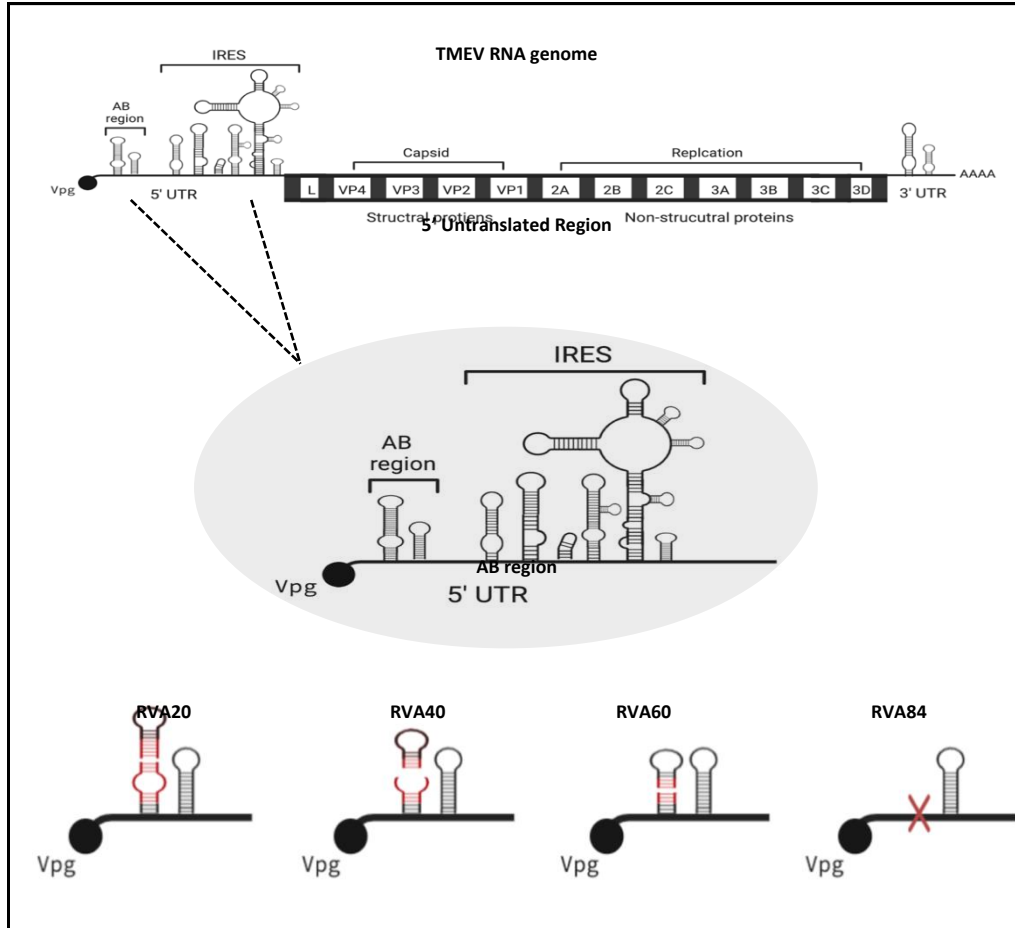
## FIGURES



**Figure 1: TMEV RNA viral genome structure.** Basic genome structure of TMEV virus. 5' untranslated region (left) with two regions of highly structured stem-loops (IRES and AB region) and capped with Vpg protein, 3' untranslated region (right) with stem-loop structure. Viral proteins (middle) divided into structural and non-structural proteins, and involved in structuring and protecting the capsid and regulating the viral replication, respectively.

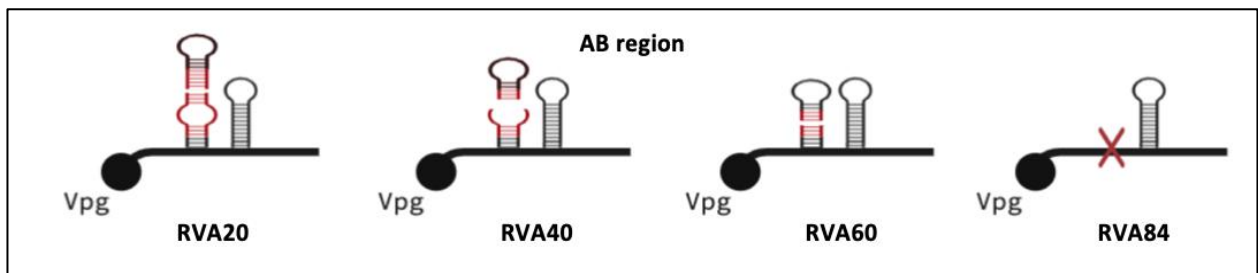
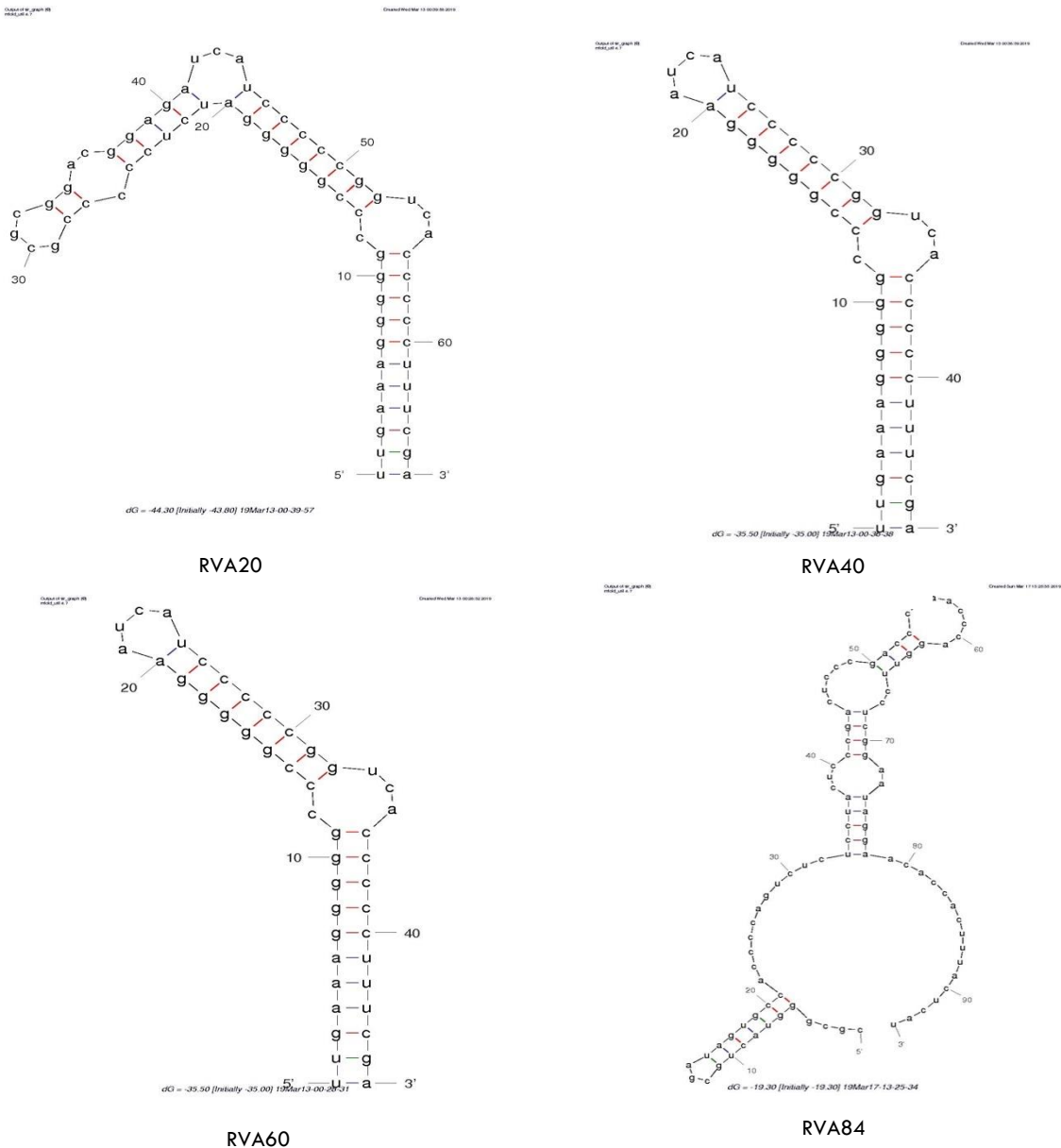


**Figure 2: Scheme for construction of plasmid pDAFI3.** pDAFI3 vector of TMEV cDNA (10.8kb) with the 5'UTR placed downstream the T7 promoter, containing restriction enzyme recognition sites for ClaI and XhoI.

**A****B****Primers:**

- **Virus #1 ( A loop)**
  - Forward primer: GCGGACGGAGATCATCCCC
  - Reverse primer: GCGGGGAGATCCCCCG
- **Virus #2 ( A loop)**
  - Forward primer: ATCATCCCCCGTCACCCC
  - Reverse primer: TCCCCGGGCCCCCTTC
- **Virus #3 ( A loop)**
  - Forward primer: GGTACCCCCCTTCGACG
  - Reverse primer: CCCCTTCAAGCCATAGTGTC
- **Virus #4 ( A loop)**
  - Forward primer: CGCGGTACTGCGATAGT
  - Reverse primer: GCCATAGTGTC AATAGTAATAAAAAGGAAAAC

**Figure 3: Design of deletions in the 5'UTR of TMEV.** **A)** Deletion design in loop A of the AB region (86nt) of the 5'UTR to generate four recombinant TMEV viruses (RV). The four RVs represent deletions of 20nt (RVA20), 40nt (RVA40), 60nt (RVA60), and 84nt (RVA84). **B)** Oligonucleotides Primers of TMEV loop A. Primers were designed to induce deletion sequences in loop A of the 5'UTR to generate four TMEV recombinant viruses.

**A****B**

**Figure 4: Secondary RNA structure of 5'UTR. A) Deletion design in the 5' UTR and B) Images from mFOLD program shows the preservation of 5'UTR loop structures.**

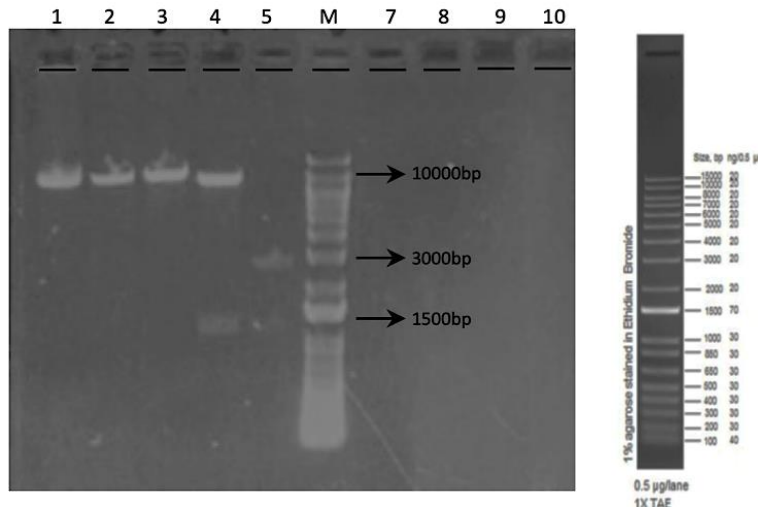


**Figure 5. Digestion of pDAFI3 and pUC75 plasmids.** Restriction enzymes XbaI and ClaI were used to digest pDAFI3 and pUC75. Digestion products of pDAFI3 and pUC75 were separated by electrophoresis using a 0.8% agarose gel. The sizes of the molecular weight standards are shown on the right (lane 6). Restriction enzymes used for the reactions correspond to pDAFI3 single digest with XbaI (lane 2), pDAFI3 single digest with ClaI (lane 3), pDAFI3 double digest with XbaI and ClaI (lane 4), and pUC75 double digest with XbaI and ClaI (lane 5). Control of wild-type TMEV pDAFI3 cDNA plasmid in lane 1. 1kb plus DNA ladder used as a molecular marker (Lane M).

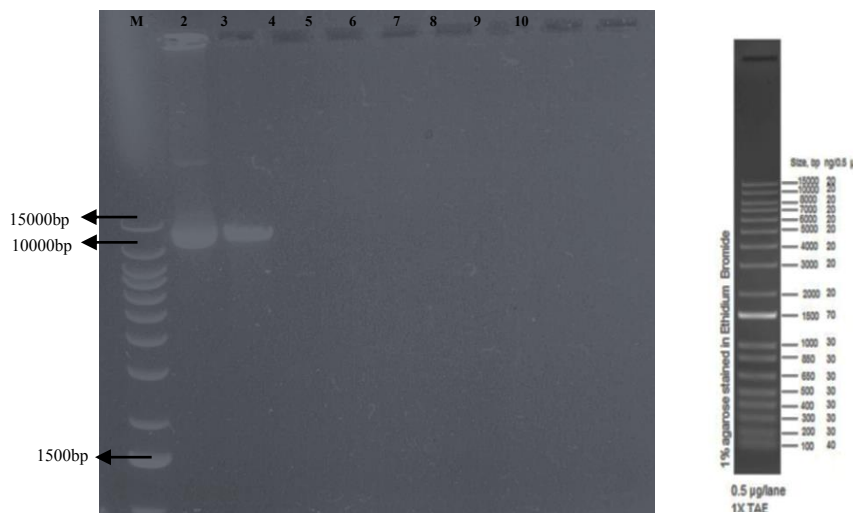


**Figure 6: Linearization of pDAFI3 plasmid.** *In-vitro* transcription was performed to purify the TMEV linear RNA product digested with XbaI. Linearized pDAFI3 product was visualized by electrophoresis using a 0.7% agarose gel. The sizes of the molecular weight standards are shown on the left (lane 1). Linear pDAFI3 product cDNA digested with XbaI (lane 3) and the control of uncut pDAFI3 (lane 2).

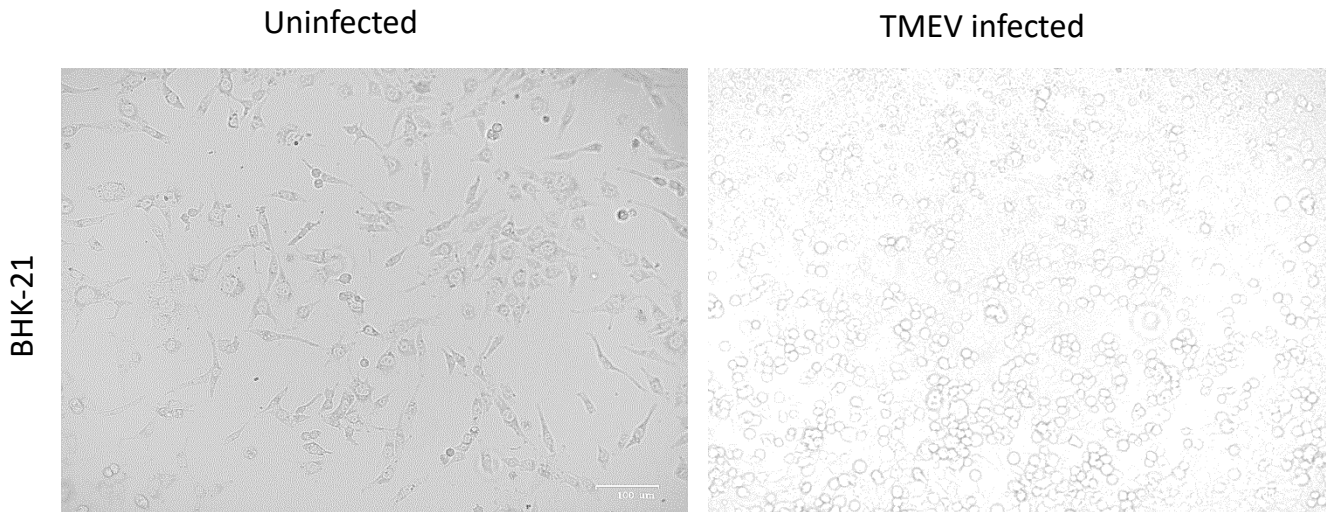


**Figure 7: Cytopathic effect of TMEV-infected BHK-21 cells.** Changes to morphology of the BHK-21 cells can be observed on the right panel, compared to a normal BHK-21 (left).

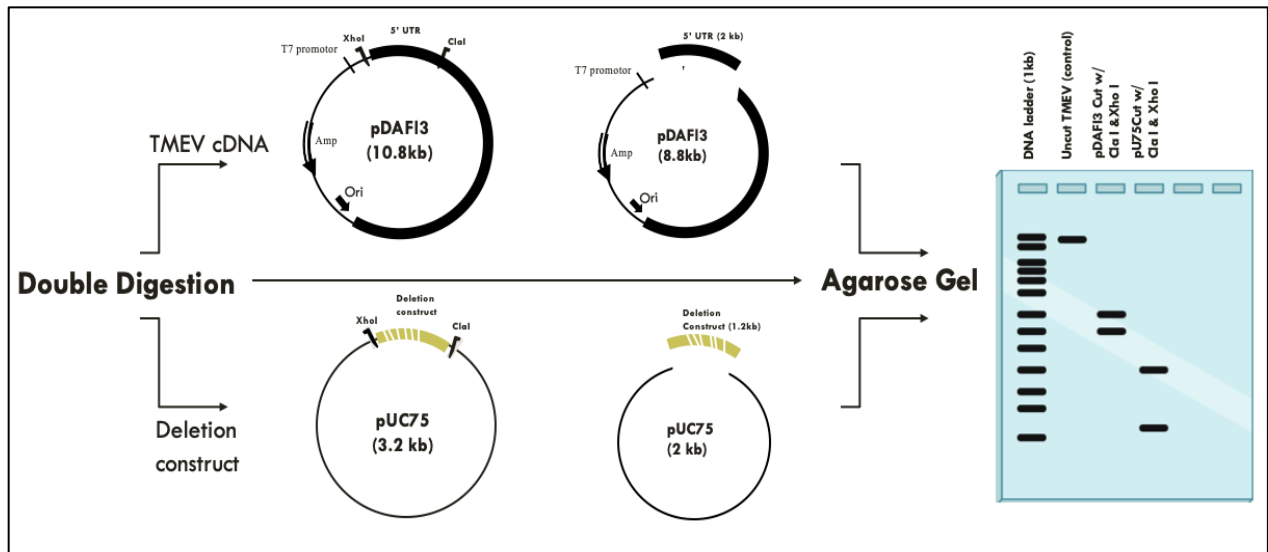


**Figure 8: Schematic representation of cloning strategy of RVA20 with construct (deletion of 20 nucleotides).**



## Reference:

1. Benjamin EJ, Blaha MJ, Chiuve SE, et al. Heart Disease and Stroke Statistics'2017 Update: A Report from the American Heart Association. *Circulation*. 2017. doi:10.1161/CIR.0000000000000485
2. Ogretmen B. Viral Myocarditis. *Physiol Behav*. 2019;176(3):139-148. doi:10.1097/BOR.0000000000000303.Viral
3. Dadashi M, Azimi T, Faghihloo E. Global study of viral myocarditis: A systematic review and meta-analysis. *J Acute Dis*. 2020;9(1):1. doi:10.4103/2221-6189.276076
4. Cooper LT, Keren A, Sliwa K, Matsumori A, Mensah GA. The global burden of myocarditis: Part 1: A systematic literature review for the global burden of diseases, injuries, and risk factors 2010 study. *Glob Heart*. 2014;9(1):121-129. doi:10.1016/j.gheart.2014.01.007
5. Garmaroudi FS, Marchant D, Hendry R, et al. Coxsackievirus B3 replication and pathogenesis. *Future Microbiol*. 2015;10(4):629-652. doi:10.2217/fmb.15.5
6. Schultz JC, Hilliard AA, Cooper LT, Rihal CS. Diagnosis and treatment of viral myocarditis. *Mayo Clin Proc*. 2009. doi:10.4065/84.11.1001
7. Siripanthong B, Nazarian S, Muser D, et al. Recognizing COVID-19–related myocarditis: The possible pathophysiology and proposed guideline for diagnosis and management. *Hear Rhythm*. 2020. doi:10.1016/j.hrthm.2020.05.001
8. Gómez RM, Rinehart JE, Wollmann R, Roos RP. Theiler's murine encephalomyelitis virus-induced cardiac and skeletal muscle disease. *J Virol*. 1996. doi:10.1128/jvi.70.12.8926-8933.1996
9. Klingel K, Hohenadl C, Canu A, et al. Ongoing enterovirus-induced myocarditis is associated with persistent heart muscle infection: Quantitative analysis of virus replication, tissue damage, and inflammation. *Proc Natl Acad Sci U S A*. 1992. doi:10.1073/pnas.89.1.314
10. Woudstra L, Juffermans LJM, van Rossum AC, Niessen HWM, Krijnen PAJ. Infectious myocarditis: the role of the cardiac vasculature. *Heart Fail Rev*. 2018. doi:10.1007/s10741-018-9688-x
11. Sin J, Mangale V, Thienphrapa W, Gottlieb RA, Feuer R. Recent progress in

- understanding coxsackievirus replication, dissemination, and pathogenesis. *Virology*. 2015;484:288-304. doi:10.1016/j.virol.2015.06.006
12. Manley G. Bioinformatics Multivariate Analysis Determined a Set of Phase- Specific Biomarker Candidates in a Novel Mouse Model for Viral Myocarditis. 2013;7(4):444-454. doi:10.1038/mp.2011.182.doi
  13. Aly M, Wiltshire S, Chahrour G, Loredó Osti JC, Vidal SM. Complex genetic control of host susceptibility to coxsackievirus B3-induced myocarditis. *Genes Immun*. 2007;8(3):193-204. doi:10.1038/sj.gene.6364374
  14. Bouin A, Nguyen Y, Wehbe M, et al. Major persistent 5' terminally deleted coxsackievirus B3 populations in human endomyocardial tissues. *Emerg Infect Dis*. 2016;22(8):1488-1490. doi:10.3201/eid2208.160186
  15. Fujioka S, Kitaura Y, Ukimura A, et al. Evaluation of viral infection in the myocardium of patients with idiopathic dilated cardiomyopathy. *J Am Coll Cardiol*. 2000. doi:10.1016/S0735-1097(00)00955-4
  16. Lindner D, Li J, Savvatis K, et al. Cardiac fibroblasts aggravate viral myocarditis: Cell specific Coxsackievirus B3 replication. *Mediators Inflamm*. 2014. doi:10.1155/2014/519528
  17. Omura S, Kawai E, Sato F, et al. Theiler's Virus-Mediated Immunopathology in the CNS and Heart: Roles of Organ-Specific Cytokine and Lymphatic Responses. *Front Immunol*. 2018. doi:10.3389/fimmu.2018.02870
  18. Huo Y, Aboud K, Kang H, Cutting LE, Bennett A. Three immune-mediated disease models induced by Theiler's virus: Multiple sclerosis, seizures and myocarditis. 2017;44(9):1-13. doi:10.1007/978-3-319-46720-7
  19. Ohara Y, Stein S, Fu J, Stillman L, Klamann L, Roos RP. Molecular cloning and sequence determination of DA strain of Theiler's murine encephalomyelitis viruses. *Virology*. 1988. doi:10.1016/0042-6822(88)90642-3
  20. Gerhauser I, Hansmann F, Ciurkiewicz M, Löscher W, Beineke A. Facets of theiler's murine encephalomyelitis virus-induced diseases: An update. *Int J Mol Sci*. 2019. doi:10.3390/ijms20020448
  21. Tang H, Pei H, Xia Q, et al. Role of gene polymorphisms/haplotypes and serum levels of interleukin-17A in susceptibility to viral myocarditis. *Exp Mol Pathol*. 2018.

doi:10.1016/j.yexmp.2018.03.002

22. Stein SB, Zhang L, Roos RP. Influence of Theiler's murine encephalomyelitis virus 5' untranslated region on translation and neurovirulence. *J Virol.* 1992.  
doi:10.1128/jvi.66.7.4508-4517.1992
23. Pevear DC, Calenoff M, Rozhon E, Lipton HL. Analysis of the complete nucleotide sequence of the picornavirus Theiler's murine encephalomyelitis virus indicates that it is closely related to cardioviruses. *J Virol.* 1987. doi:10.1128/jvi.61.5.1507-1516.1987
24. Oka K, Oohira K, Yatabe Y, et al. Fulminant myocarditis demonstrating uncommon morphology-a report of two autopsy cases. *Virchows Arch.* 2005. doi:10.1007/s00428-004-1173-3